AD-756 176

ADAPTATION OF THE NRL ACOUSTIC RESEARCH TANK FACILITY FOR EXPERIMENTS IN PARAMETRIC SONAR, WITH PRELIMINARY RESULTS

Anthony I. Eller

Naval Research Laboratory
Washington, D. C.

29 January 1973

Adaptation of the NRL Acoustic Research Tank Facility for Experiments in Parametric Sonar, with Preliminary Results

ANTHONY I. ELLER

Naval Postgraduate School

and

Transducer Branch
Acoustics Division

January 29, 1973

NAVAL RESEARCH LABORATORY
Washington, D.C.

DOCUMENT CONTROL DATA - R & D

(Security classification of title, body of abstract and indexing annotation must be entered when the overall report is classified)

1. ORIGINATING ACTIVITY (Corporate author)	2a. REPORT SECURITY CLASSIFICATION
Naval Research Laboratory Washington, D.C. 20375	Unclassified
	2b. GROUP

3. REPORT TITLE

ADAPTATION OF THE NRL ACOUSTIC RESEARCH TANK FACILITY FOR EXPERIMENTS IN PARAMETRIC SONAR, WITH PRELIMINARY RESULTS

4. DESCRIPTIVE NOTES (Type of report and inclusive dates)
An interim report on a continuing NRL Problem.

5. AUTHOR(S) (First name, middle initial, last name)

Anthony I. Eller

6. REPORT DATE	7a. TOTAL NO. OF PAGES	7b. NO. OF REFS
January 29, 1973	28 24	7

8a. CONTRACT OR GRANT NO.	9a. ORIGINATOR'S REPORT NUMBER(S)
b. PROJECT NO. SF11121-103, Task No. 13728 and	NRL Report 7513
c. Project No. SF11121-601, Task No. 16727	9b. OTHER REPORT NO(S) (Any other numbers that may be assigned this report)
d.	

10. DISTRIBUTION STATEMENT

Approved for public release; distribution unlimited.

11. SUPPLEMENTARY NOTES	12. SPONSORING MILITARY ACTIVITY
Details of illustrations in this document may be better studied on microfiche.	Department of the Navy (Naval Ship Systems Command), Washington, D.C. 20360

13. ABSTRACT

The NRL Acoustic Research Tank Facility, with its capability for obtaining numerical planar scans and graphic recordings of radiation patterns, has been adapted for use in parametric sonar studies. In a preliminary set of experiments, the facility was used to study difference-frequency radiation from an acoustic parametric source. The source utilized a USRD type E8 transducer, driven simultaneously at two frequencies close to the resonance frequency of 1.5 MHz. This report describes the experimental apparatus and illustrates the flexibility of the tank facility as a research tool in nonlinear acoustics. It also presents measured values of the difference-frequency sound pressure level and a sequence of radiation patterns that illustrates beam formation in the near field of the parametric source.

14 KEY WORDS	LINK A		LINK B		LINK C	
	ROLE	WT	ROLE	WT	ROLE	WT
Nonlinear acoustics						
Parametric sonar						
Difference frequency						

DD FORM 1 NOV 65 1473 (BACK)

(PAGE 4)

CONTENTS

i-C

ABSTRACT

The NRL Acoustic Research Tank Facility, with its capability for obtaining numerical planar scans and graphic recordings of radiation patterns, has been adapted for use in parametric sonar studies. In a preliminary set of experiments, the facility was used to study difference-frequency radiation from an acoustic parametric source. The source utilized a USRD type E8 transducer, driven simultaneously at two frequencies close to the resonance frequency of 1.5 MHz. This report describes the experimental apparatus and illustrates the flexibility of the tank facility as a research tool in nonlinear acoustics. It also presents measured values of the difference-frequency sound pressure level and a sequence of radiation patterns that illustrates beam formation in the near field of the parametric source.

PROBLEM STATUS

This is an interim report on a continuing NRL Problem.

AUTHORIZATION

SYMBOLS

A	area of active part of transducer face
c	speed of sound
f_d, f_1, f_2	difference frquency and primary frequencies
f_0	primary center frequency, $(f_1 + f_2)/2$
M_e	free-field voltage sensitivity
P_{ref}	reference pressure used in defining decibels
R	range
R_0	primary-wave Fresnel distance, Af_0/c
R_d	difference-frequency Fresnel distance, Af_d/c
S_i	transmitting current response
SL	source level referred to distance of $1m$ (in dB re 1 μPa)
SL_1, SL_2, SL_d	value of SL for each primary frequency and difference frequency
SPL	sound pressure level (in dB re 1 μPa)
SPL_{01}, SPL_{02}	values of SPL in the collimated near field of each primary component
SPL_d	value of SPL for difference-frequency component
α_0	attenuation coefficient at primary center frequency
β	nonlinearity parameter of water
ρ	density of water
λ	wavelength of sound in water

ADAPTATION OF THE NRL ACOUSTIC RESEARCH TANK FACILITY FOR EXPERIMENTS IN PARAMETRIC SONAR, WITH PRELIMINARY RESULTS

INTRODUCTION

An acoustic parametric source has been assembled and operated in conjunction with the NRL Acoustic Research Tank Facility. The source utilizes a single USRD type E8 transducer, driven simultaneously by two sinusoidal current components of equal amplitude at frequencies close to the resonance frequency of 1.5 MHz. Because of the nonlinear nature of acoustic propagation, the two high-frequency primary signals mix within the medium to generate narrow-beam radiation at the difference frequency. The maximum electrical power delivered to the source in both frequency components together is about 6 W. At this power level each primary acoustic signal has a nominal source level of 204 dB re 1 μPa at 1 m. Typical difference frequencies range from 25 to 200 kHz. Other descriptions of difference-frequency generation by an acoustic parametric source are found in the reports that are listed in the Bibliography.

The first section of this report describes the experimental equipment and some of the problems associated with its use; the second section describes the performance of the parametric source.

DESCRIPTION OF EQUIPMENT

Electronic Equipment

The experimental arrangement was developed in the upper tank facility at NRL, which has a cylindrical wooden tank, 20 ft in diameter and 22 ft deep. A block diagram of the equipment is shown in Fig. 1. The equipment inside the dashed line is part of a measurement system that was installed by Scientific Atlanta, Inc. Items outside the dashed line represent additional equipment needed to augment the system.

Transmitting System—Two high-frequency primary components are supplied by two separate oscillators. An electronic frequency counter is available to measure either frequency. Cables from each oscillator lead to the input tap on the front of a Scientific Atlanta line driver which is part of the original installation. The driving signal next passes through a signal gate and then to an attenuator, which is connected into the circuit by means of a patch cable from the XMTR OUT to the ATTENUATOR IN taps on the control panel. A cable from the ATTENUATOR OUT tap then takes the driving signal to the GR1233A power amplifier and from there to the E8 transducer. A high-pass filter has been added to the output of the power amplifier to block the slight amount of difference-frequency current that is generated within the amplifier. The filter is a T network consisting of two 0.0033-μF capacitors and a 3.5-μH inductor to ground.
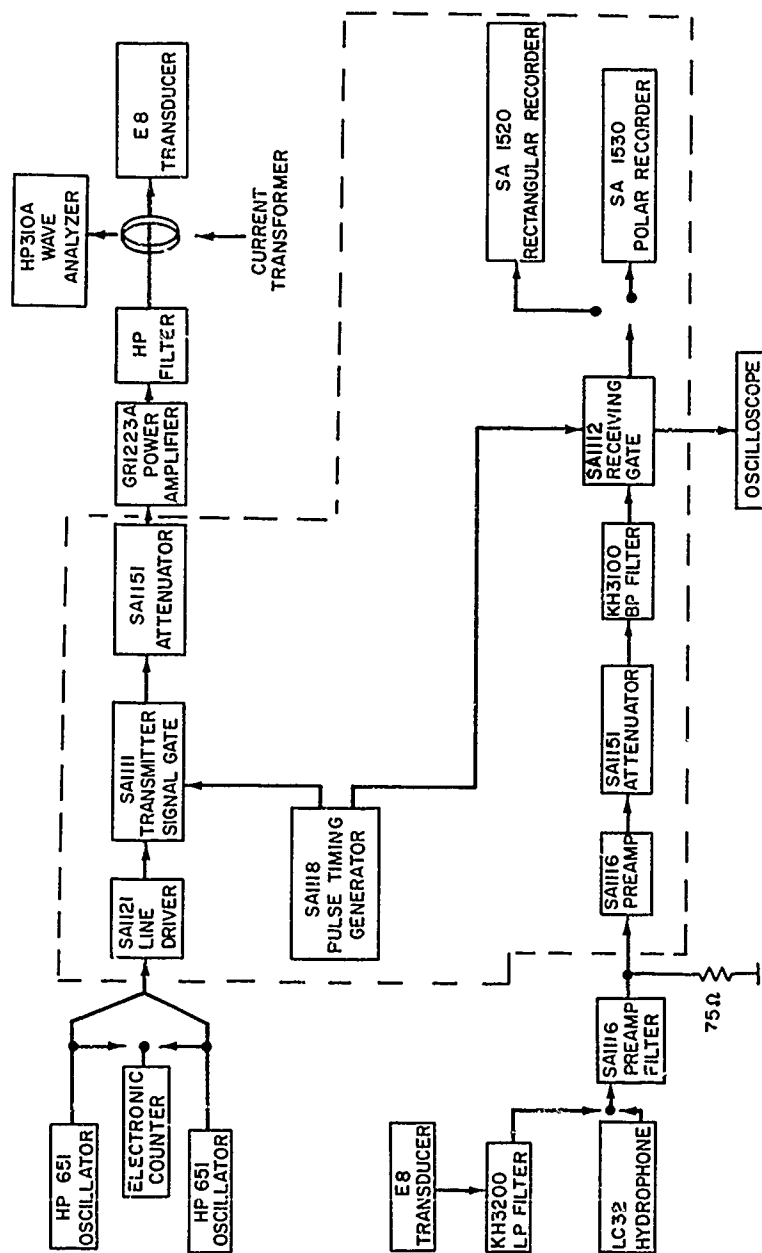
1

ANTHONY I. ELLER

Fig. 1—Experimental equipment

The rms amplitude of each primary component of the driving current is measured by means of a Pearson Electronics Current Transformer looped about one wire leading to the transducer. The current transformer produces a voltage, proportional to the current, that is measured with a Hewlett Packard Model 310A Wave Analyzer during cw operation of the transducer. In some cases, when the power amplifier was operated at close to its maximum level, the current amplitude during pulsed operation was slightly greater than during cw operation. In these cases the amplitude of a current pulse was determined by comparing the pulsed and cw signals on the oscilloscope and then adjusting accordingly the cw amplitude read from the wave analyzer.

Receiving System—The receiving hydrophone, which is either an LC32 used alone or an E8 used with a Krohn-Hite 3200 low-pass filter, is connected to a Scientific Atlanta 1116 combined preamplifier and filter unit. This preamplifier and filter unit is needed in addition to the preamplifier in the Scientific Atlanta installation to help raise the relatively weak difference-frequency signals to a level of 1 V, needed to drive the recorders. The added Krohn-Hite filter was used only in connection with the E8 hydrophone; it blocked the high-frequency primary signals more effectively than did the filters within the 1116 preamplifier and filter unit alone. The Krohn-Hite filter was unnecessary with an LC32 hydrophone because that hydrophone is insensitive to the high-frequency components.

The received signal enters the Scientific Atlanta installation at the SIGNAL IN tap on the control panel. Because the preamplifiers are designed to feed into a 75-ohm load, a 75-ohm resistor was connected across the output of the first preamplifier. The preamplifier, attenuator, filter, gate, and recorder within the Scientific Atlanta installation are interconnected by means of patch cables on the control panel. The input and output impedances of all Scientific Atlanta equipment are 75 ohms except for the high input impedance of the preamplifier. The input and output impedances of the Krohn-Hite bandpass filter were modified during its original installation so that one may choose to include or bypass it without altering the nominal gain of the receiving system. As modified, the input and output impedances of the Krohn-Hite filter are 75 and 4 ohms.

A pulse timing generator to trigger the transmitting and receiving gates and a servomechanism to rotate the transducer and to control the motion of the graphic recorders are also part of the Scientific Atlanta installation.

Properties of Transducers

Parametric sound generation was accomplished with the USRD type E8#50 transducer. The E8 transducer operates in the frequency range from 100 to 2000 kHz, with a resonance at approximately 1450 kHz. The 3-dB bandwidth of the resonance peak is about 250 kHz. The active element of the transducer is a disk of lithium sulfate 2 cm in diameter, and the nominal electrical input resistance at resonance is 50 ohms. The E8 transducer is driven by two sinusoidal current components at frequencies close to resonance; it thus generates two primary acoustic waves that mix nonlinearly in the water to form a difference-frequency wave. Each primary wave consists, approximately, of a near-field collimated plane wave of cross-section diameter equal to that of the radiating disk and extending to the Fresnel distance $R_0 = A/\lambda$, and a far-field portion whose amplitude is inversely proportional to range. The level of each primary component is expressed either in terms of an average amplitude of the near-field collimated wave, or in terms of the source level, which is the far-field *SPL* extrapolated to a range of 1 m. Either quantity is determined from the transmitting current response, which in turn is calculated from the transducer's free-field voltage sensitivity M_e and the plane-wave or spherical-wave reciprocity

parameter (1). A calibration curve for transducer E8#50, giving M_e as a function of frequency, was supplied by the Underwater Sound Reference Division, Orlando, Fla. Part of the curve is reproduced in Fig. 2a. The free-field voltage sensitivity at resonance is -201 dB re 1V/μPa.

The transmitting current response at resonance for the average pressure in the near-field region is given by the reciprocity relation

$$20 \log S_i \; = \; 20 \log M_e \; + \; 20 \log \left(\frac{\rho c}{2A} \right) \; = \; 226 \text{ dB re } 1 \; \mu\text{Pa/A.}$$

Similarly, the transmitting current response at resonance for the far field at a range $R = 1$ m is

$$20 \log S_i \; = \; 20 \log M_e \; + \; 20 \log \left(\frac{\rho c}{2R\lambda} \right) \; = \; 216 \text{ dB re } 1 \; \mu\text{Pa/A.}$$

The *SPL* of each primary wave is shown against range in Fig. 2b, where it is assumed that transducer E8#50 is driven at resonance with a current of 1 A. The averaged near-field *SPL* is flat in the region extending to 0.30 m, where the far-field response begins. More information concerning the E8 transducer is available in a USRD instruction book (2) and in Ref. 3.

(a) M_e for transducer E8#50

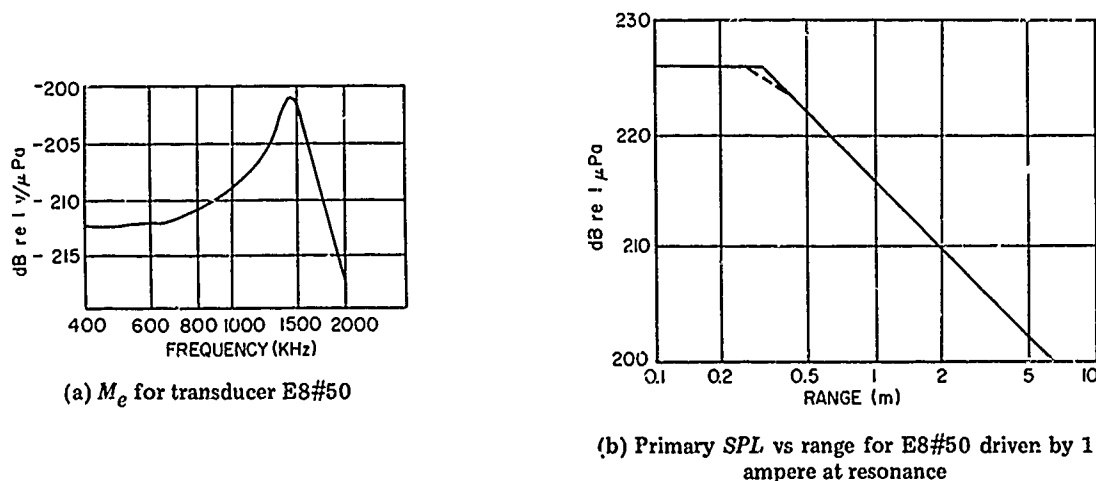(b) Primary *SPL* vs range for E8#50 driven by 1 ampere at resonance

Fig. 2—Properties of primary radiation

A second E8 transducer, #43, was used to receive the primary acoustic signals as well as difference-frequency signals above 100 kHz. The free-field voltage sensitivity of E8#43 at resonance is -200 dB re 1 V/μPa. As a check on the calibration and performance of the two E8 transducers, a cw 1410-kHz signal was transmitted from E8#50 to E8#43, over a range of 3.7 m. The predicted *SPL* at 3.7 m was computed from the measured current and the transmitting current response of E8#50, including the effects of spherical spreading and absorption, and was compared to the received *SPL*, as computed from the measured voltage and the free-field voltage sensitivity of E8#43. The two values of *SPL* agreed to

within 1.2 dB. All values of primary level stated in this report are based on current measurements, and there is an uncertainty of perhaps 2 dB.

A model LC32 hydrophone was also used to receive difference-frequency signals, generally below 100 kHz.

Measurements of the difference-frequency *SPL* require having a reliable calibration of the receiving hydrophones. Therefore, a reciprocity calibration of the free-field voltage sensitivity of the two hydrophones was performed in the upper tank at frequencies of 50, 100, and 200 kHz. The results appear in Table 1.

Table 1
Receiving Voltage Sensitivity of the Hydrophones

Hydrophone	Frequency (kHz)	$20 \log M_e$ (dB re 1 V/μPa)
LC32	50	-208
LC32	100	-216
E8#43	100	-212
E8#43	200	-213

Problems with Noise

In order to obtain acceptable radiation distribution patterns, it is necessary to have as high a signal-to-noise ratio as possible. One way to increase the signal-to-noise ratio is to drive the source at its maximum signal level. Consequently, most radiation distribution patterns were plotted when driving the parametric source near its maximum current of about 0.25 A in each primary component. Attempts to further increase the current led to a distorted current waveform with no increase in acoustic signal.

To further increase the signal-to-noise ratio one must eliminate unnecessary electrical noise. For example, because the Krohn-Hite #3200 filter appeared to be a source of electrical noise, it was used only in connection with the E8#43 hydrophone, where its use was essential, and was removed from the circuit when the LC32 hydrophone was used. Because of the noise introduced by active filters, the Parametric Sonar Group at NUSC, New London, advocates the use of passive filters in the receiving system.

An indiscriminate setting of gain and filtering controls in the receiving network generally yields a less than optimal signal-to-noise ratio. The best signal-to-noise ratios, and consequently the best-looking radiation distribution patterns, were obtained with the following control settings in the receiving network. These settings are specified for receiving a 50-kHz signal with the LC32 hydrophone:

SA1116 Preamplifier and filter: 30 dB gain, 3- to 150-kHz passband

SA1116 Preamplifier: 40 dB gain

Band-pass Filter: 25- to 100-kHz passband.

The attenuator was used to reduce the received signal to the required 1 V for the recorder.

Reverberation was generally not a problem during pulsed operation. In one case, however, radiation patterns at 50 kHz, taken in the main tank at ranges of 4.1 and 5.3 m, showed some unexpected sidelobes about 30 dB below the axial level. The sidelobes disappeared when the pattern was replotted at a lower pulse repetition rate. The results suggest that the sidelobes were due to reverberation, and one can infer that reverberation is not likely to be a problem unless one is looking at pressure levels 30 dB below the axial level.

Another noise problem is the presence of a periodic noise spike in the receiving network that could drastically alter the appearance of a radiation pattern. The origin of the noise spike is not known at present. Fortunately it is related to the line frequency and can be screened from the receiving signal gate by an appropriate adjustment of pulse repetition rate during visual monitoring of the received signal.

Problems of broadband electrical noise, reverberation, and noise spikes were not important in measurements of axial pressure levels. Noise problems became significant during measurement of off-axis signals, where the pressure level was 20 dB or more below the axial level.

Other Sources of Nonlinearity

The basis of the acoustic parametric source is the nonlinearity that is inherent in acoustic propagation. The associated electronic system, however, contains two additional possible sources of nonlinearity that can interfere with observation of the desired results.

One source of nonlinearity is the power amplifier, where the high-frequency primary signals mix to create a small signal component at the difference frequency. During some early experimental runs, the power amplifier was connected directly to the E8 transducer, without use of the high-pass filter; consequently, a small difference-frequency current was present which caused some direct radiation of sound at the difference frequency. These results are described in Appendix A. When the high-pass filter is connected to the output of the power amplifier, no component at the difference frequency could be detected in the current to the transducer, and the resulting radiation levels and directivity patterns show no observed indication of the presence of direct radiation.

A second source of nonlinearity is the SA1116 preamplifier and filter unit in the receiving network. At the available hydrophone locations, the received acoustic signal contains high-frequency components that are typically 60 dB greater than the difference-frequency component. It is necessary to block the high-frequency signal by suitable filtering before amplifying the relatively weak difference-frequency signal. If the high-frequency components are not sufficiently attenuated, their presence will saturate the preamplifier and lead to difference-frequency generation within the preamplifier. This spurious form of difference-frequency generation is easily recognized, however, because its dependence on angle and range is closely related to that of the primary signal. The SA1116 preamplifier and filter unit consists of a series of amplification and filtering stages whose order of appearance depends on the gain setting control. For some gain settings all amplification occurs before the filtering, and unless filtering has been obtained by some other means, the high-frequency components are then likely to saturate the amplifier and cause difference-frequency generation. An added convenience of the LC32 hydrophone is that it is

insensitive to the high frequencies and thus performs most of the necessary high-frequency filtering itself. When the E8#43 transducer is used as a hydrophone, it is necessary to include the KH3200 low-pass filter at the head of the receiving network in order to achieve adequate high-frequency rejection.

PERFORMANCE OF THE ACOUSTIC PARAMETRIC SOURCE

The sound pressure level of the radiated difference-frequency signal was measured on-axis at various ranges and for various values of primary and difference frequencies. In addition, polar and rectangular radiation patterns were obtained for various conditions. The results are summarized in the following subsections.

Sound Pressure Level vs Range

The difference-frequency sound pressure level SPL_d is shown as a function of range in Fig. 3. The primary frequencies for this situation were 1410 and 1460 kHz, giving a difference frequency of 50 kHz. The E8 transducer was operated in a pulsed mode, and each of the two primary acoustic waves had a near-field sound pressure level of 214 dB re 1 μPa, as computed from the near-field current response of transducer E8#50. The points O indicate a set of measurements made in the upper tank; the points Δ indicate the results of a supposedly identical situation in a second tank. The two sets of data indicate the degree of reproducibility that can be expected.

The dashed curve in Fig. 3 represents an extrapolation inward of Westervelt's asymptotic result (4), valid far from the source, which can be written as
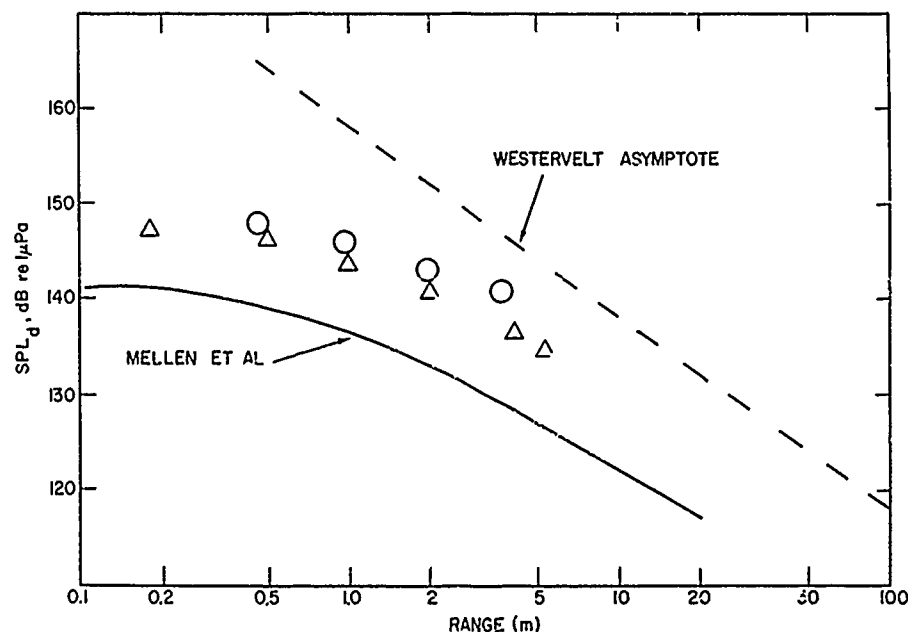

Fig. 3—Sound pressure level at difference frequency of 50 kHz vs range

$$SPL_d = SPL_{01} + SPL_{02} + 40 \log f_d + 20 \log \frac{\sqrt{2}\beta\pi AP_{\text{ref}}}{\rho c^4} - 20 \log 2\alpha_0 R, \quad (1)$$

where

$$SPL_{01} = SPL_{02} = 214 \text{ dB}$$

$$f_d = 50 \text{ kHz}$$

$$\beta = 3.6$$

$$\rho = 10^3 \text{ kg/m}^3$$

$$c = 1480 \text{ m/s}$$

$$A = 3.2 \times 10^{-4} \text{ m}^2$$

$$P_{\text{ref}} = 1 \mu\text{Pa}$$

$$\alpha_0 = 0.04 \text{ Np/m}.$$

It is noted that the primary levels are chosen to agree with the near-field levels of the experiment.

The lower curve in Fig. 3 is based upon an analytic result of Mellen, Browning, and Konrad (5) which is written as

$$SPL_d = SPL_{01} + SPL_{02} + 40 \log f_d + 20 \log \frac{\sqrt{2}\beta\pi AP_{\text{ref}}}{\rho c^4}$$

$$+ 20 \log \left[\frac{\ell_n \left(1 + \dfrac{R}{R_d} \right)}{\left(1 + \dfrac{R}{R_0} \right)} \right]. \quad (2)$$

A misprint in Ref. 5 has been corrected in the above expression. The values in the calculations are the same as those used for the Westervelt result, with the addition of $f_0 = 1.4 \times 10^6$ Hz used in the calculation of R_0.

The acoustic attenuation of the primary frequencies is $\alpha_0 = 0.04$ Np/m, and according to the Westervelt model, the effective length $(1/2\alpha_0)$ of the array is 12.5 m. Difference-frequency generation, therefore, is occurring throughout the range represented in Fig. 3. Consequently, the difference-frequency pressure amplitude decreases more slowly than $1/R$, or -20 dB per decade. A reliable estimate of the effective length of the array for diverging primaries is not known. According to the present results, the effective array length certainly exceeds the Fresnel length, $R_0 = 0.30$ m, of the collimated portion of the primary beam.

A rough estimate of the difference-frequency source level for the driving conditions of the experiment can be obtained from the measured SPL_d at 5.3 m, referred to a distance of 1 m, by means of the relation

$$SL_d = SPL_d(5.3 \text{ m}) + 20 \log 5.3 = 149 \text{ dB re } 1 \text{ } \mu\text{Pa}.$$

A more accurate value of SL_d would require far-field measurements of SPL_d.

Nonlinear Conversion Parameter

The sound pressure level of difference-frequency signals was measured at frequencies of 50, 100, and 200 kHz at a range of 3.7 m. The theoretical results in Eqs. (1) and (2) indicate that the difference-frequency pressure amplitude is proportional to the square of the primary pressure amplitude. Accordingly, it is convenient to normalize the results for SPL_d by introducing a nonlinear conversion parameter, defined as $SPL_d - SPL_{01} - SPL_{02}$. This parameter is a measure of the coupling into the difference-frequency component. Values of the difference frequency f_d, the primary center frequency f_0, and the nonlinear conversion parameter are presented in Table 2. From the degree of repeatability of the results and the uncertainty of calibration, the values of the conversion parameter are considered valid to within 2 dB. When the difference frequency changes from 50 to 200 kHz, the nonlinear conversion parameter in Table 2 increases by 14 dB. In contrast, the Westervelt result, Eq. (1), predicts that far-field values of the conversion parameter increase with frequency at a rate of 12 dB per octave, for a total increase of 24 dB over the range 50 to 200 kHz. Equation (2) includes near-field effects and predicts an increase of about 11 dB per octave, for a total increase of 22 dB, at a range of 3.7 m. Neither equation adequately accounts for the observed increase of 14 dB over this frequency range.

Table 2
Nonlinear Conversion Parameter at 3.7 m

f_d (kHz)	f_0 (kHz)	$(SPL_d - SPL_{01} - SPL_{02})$ dB re $(1 \text{ } \mu\text{Pa})^{-1}$
50	1435	-287
100	1450	-278
200	1400	-273

Radiation Distribution Patterns

Polar and rectangular radiation distribution patterns were plotted with the automatic recording equipment that is part of the Scientific Atlanta installation. Typical radiation patterns are shown in Figs. 4 through 7. In obtaining each of these plots, direct radiation at the difference frequency, due to nonlinear mixing within the power amplifier, was prevented by use of the high-pass filter at the amplifier output.

Figure 4 is a sequence of polar radiation distribution patterns at ranges from 0.5 to 3.7 m of a parametrically generated difference-frequency beam at 50 kHz. These patterns illustrate the gradual formation of the beam as a function of range. The pattern at 0.5 m is noticeably broader than the others, and the patterns at 2.0 and 3.7 m are nearly identical.
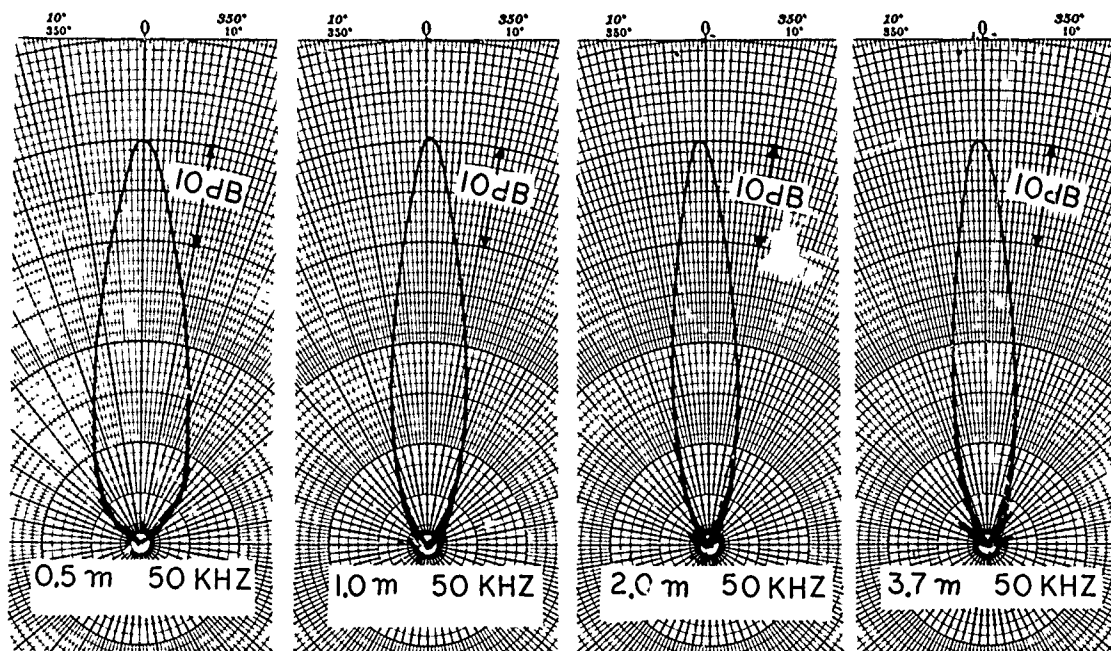
Fig. 4—Difference-frequency radiation patterns at 50 kHz for a sequence of ranges
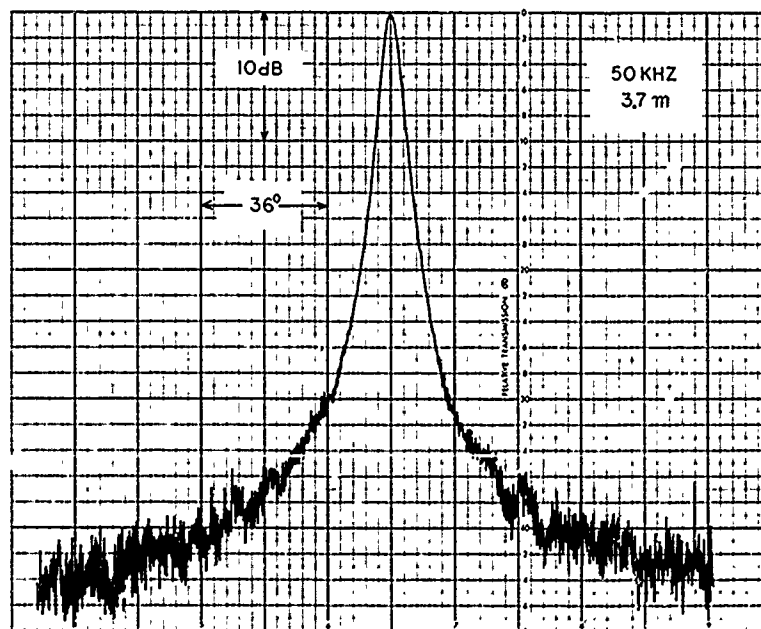
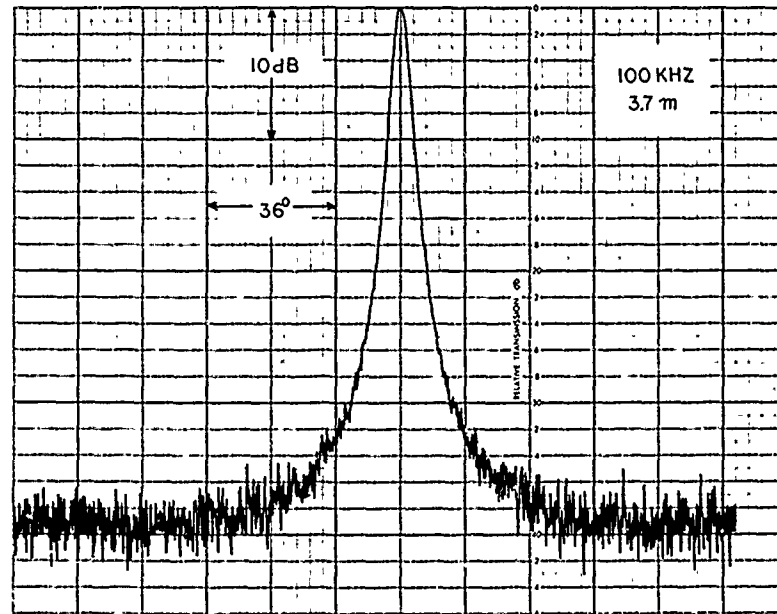Fig. 5—Rectangular difference-frequency radiation pattern at 50 kHz

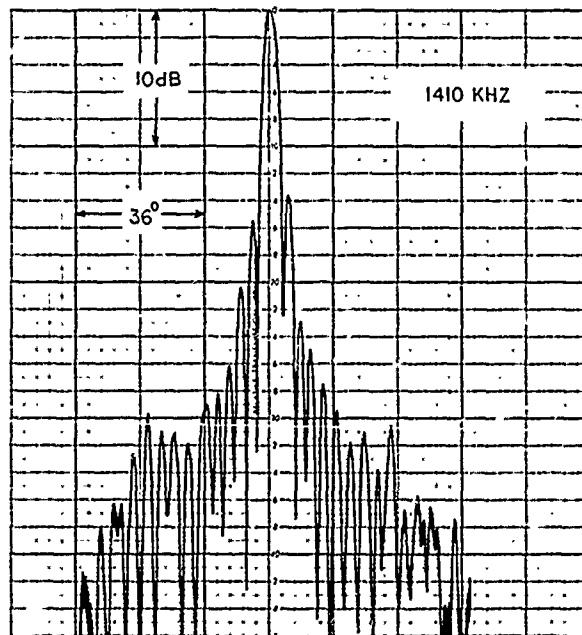Fig. 6—Rectangular difference-frequency radiation pattern at 100 kHz

Fig. 7—Rectangular primary radiation pattern

All patterns refer to the same acoustic field; the attenuator in the receiving network was adjusted so that the peak of each plotted pattern has the same position on the graph.

Figures 5 and 6 compare rectangular (i.e., xy-plotted) radiation patterns at frequencies of 50 and 100 kHz at the same range of 3.7 m. The pattern at 100 kHz is somewhat narrower than that at 50 kHz. Otherwise, doubling the difference frequency appears to have little effect on the radiation pattern at this range.

Figure 7 is a rectangular radiation pattern of one of the primary components. A comparison of Fig. 7 with Figs. 5 and 6 shows that the major part of the primary beam is narrower than either of the difference-frequency beams.

Figure 8 is an automatic scan of a planar cross section of the difference-frequency pressure field at close range. The ability to obtain this type of acoustic scan is a unique feature of the NRL Acoustic Research Tank Facility and is described in Ref. 6. Each number printed in the graph indicates the sound pressure level in decibels below the axial level. To better illustrate the contours of equal pressure level, only the even-numbered pressure levels are printed. This scan was made with an LC10 hydrophone mounted in an end-on position. Figure 8 indicates that, as anticipated, the difference-frequency pressure field is symmetrical about the axis.

Beamwidth vs Frequency and Range

The angular width of the radiation patterns at points 3 dB, 6 dB and 10 dB below the axial level was determined from plotted radiation patterns. It was found convenient to use rectangular patterns with a horizontal scale of $0.6°$ per small division for this purpose. With the help of an architect's scale, the beamwidths could be read to the nearest $0.1°$. The resulting beamwidths of difference-frequency radiation patterns are given in Tables 3 and 4. Table 3 gives beamwidths at various frequencies at a range of 3.7 m. Table 4 gives beamwidths at 50 kHz as a function of range. The slight discrepancy in measured beamwidths for 50 kHz at 3.7 m, seen in comparing the second line of Table 3 and the last line of Table 4, is indicative of the level of consistency of the results. The measured 3-dB beamwidths may be compared to the 3-dB beamwidth predicted by Westervelt's (4) model for the far field of a parametric source, given by

$$\text{3-dB beamwidth} = 2\left(\frac{2\alpha_0 c}{\pi f_d}\right)^{1/2}.$$

For f_d = 50 kHz and α_0 = 0.04 Np/m, this equation gives $3.15°$, which is less than the measured result of $4.0°$. The reason for the larger observed beamwidths is not known. However, the assumptions underlying the Westervelt model are not satisfied by the experimental conditions, and close agreement between calculated and measured beamwidths is not anticipated. Other experimenters, e.g., Smith (7), have measured 3-dB beamwidths that are narrower than the results predicted by the Westervelt formula.
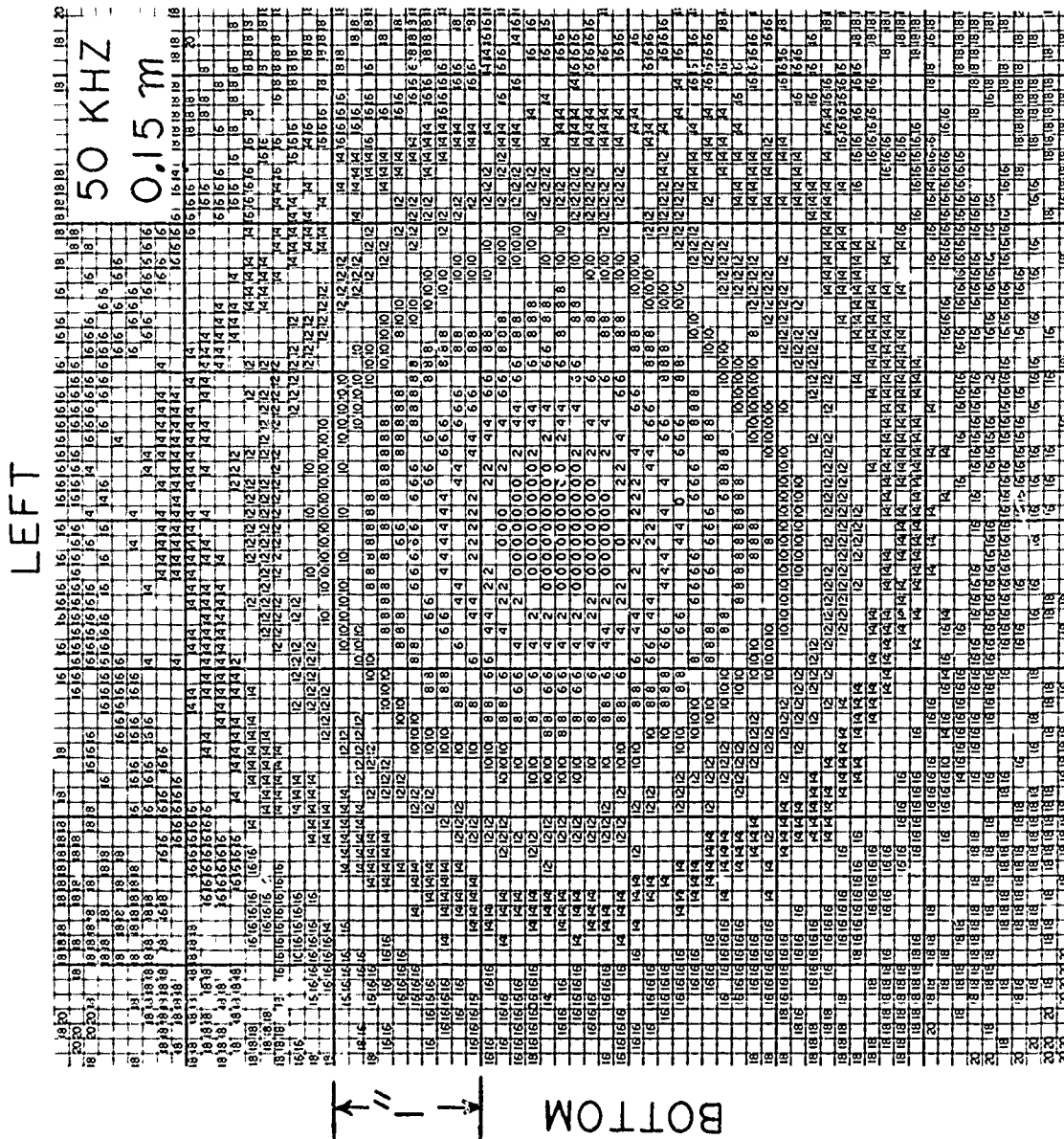
TOP

Fig. 8—Automatic scan of difference-frequency radiation

Table 3
Beamwidths of Difference-Frequency Radiation Patterns at 3.7 m
for Various Difference Frequencies

Frequency (kHz)	Beamwidth (degrees)		
	-3 dB	-6 dB	-10 dB
25	4.5	6.8	10.5
50	4.0	5.8	8.4
100	3.6	5.2	7.1
200	3.4	4.7	6.5

Table 4
Beamwidths of Difference-Frequency Radiation Patterns at
50 kHz for various Ranges

Range (m)	Beamwidth (degrees)		
	-3 dB	-6 dB	-10 dB
0.5	4.9	7.9	12.8
1.0	4.2	6.5	10.0
2.0	4.1	5.9	9.1
3.7	4.1	5.9	8.6

Summary of Typical Operating Characteristics

The typical operating characteristics of the E8 parametric sound source are summarized for operation at maximum level for a difference frequency to 50 kHz.

1. Transducer Properties

   Piston radius $a = 0.01$ m

2. Driving Signal

   Frequencies = 1410 kHz, 1460 kHz
   Rms current = 0.25 A in each primary component
   Total rms current = 0.35 A
   Pulsed mode of operation
   Peak electrical power (based on nominal input resistance of 50 ohms) = 6 W

3. Primary Acoustic Waves

    Nearfield primary pressure, $SPL_{01} = SPL_{02} = 214$ dB re 1 μPa
    Primary source level, $SL_1 = SL_2 = 204$ dB re 1 μPa, referred to 1 m
    Primary 3-dB beamwidth (measured at 1410 kHz) = $3.6°$
    Primary wave Fresnel length $R_0 = 0.30$ m
    Calculated array length $(1/2\alpha_0) = 12.5$ m

4. Difference-Frequency Signal

    Frequency = 50 kHz
    SPL_d (at 5.3 m) = 135 dB re 1 μPa
    Estimated source level (based on SPL_d at 5.3 m for the driving signal specified above) = 149 dB re 1 μPa, referred to 1 m
    3-dB beamwidth (best value at 3.7 m) = $4.0°$
    Fresnel length $R_d = 0.011$ m
    Comparison of primary and difference-frequency source levels: $SL_d - SL_1$ = –55 dB.

REFERENCES

1. W. J. Trott, "Reciprocity Parameters Derived from Radiated Power," J. Acoust. Soc. Amer. 34, 989-990 (L) (1962).

2. "USRD Type E8 Transducer," NRL Instruction Book No. 94, USRD Orlando, Fla. (1971).

3. R. J. Bobber, *Underwater Electroacoustic Measurements*, Naval Research Laboratory, Washington, D.C. 1970, pp. 266-269.

4. P. J. Westervelt, "Parametric Acoustic Array," J. Acoust. Soc. Amer. 35, 535-537 (1963).

5. R. H. Mellen, D. G. Browning, and W. L. Konrad, "Parametric Sonar Transmitting Array Measurements," J. Acoust. Soc. Amer. 49, 932-935 (L) (1971).

6. J. Chervenak, "A New NRL Acoustic Research Tank Facility," NRL Report No. 6822, Feb. 14, 1969.

7. B. V. Smith, "An Experimental Study of a Parametric End-Fire Array," J. Sound Vib. 14, 7-21 (1971).

BIBLIOGRAPHY

The following is a partial listing of papers related to this report.

J. L. S. Bellin and R. T. Beyer, "Experimental Investigation of an End-Fire Array," J. Acoust. Soc. Amer. 34, 1051-1054 (1962).

H. O. Berktay, "Possible Exploitation of Nonlinear Acoustics in Underwater Transmitting Applications," J. Sound Vib. 2, 435-461 (1965).

H. O. Berktay, "Near-Field Effects in Parametric End-Fire Arrays," J. Sound Vib. 20, 135-143 (1972).

H. Hobaek, "Experimental Investigation of an Acoustical End-Fire Array," J. Sound Vib. 6, 460-463 (1967).

R. H. Mellen, D. G. Browning, and W. L. Konrad, "Parametric Sonar Transmitting Array Measurements," J. Acoust. Soc. Amer. 49, 932-935 (L) (1971).

R. H. Mellen, W. L. Konrad, and D. G. Browning, "Approximate Scaling Laws for Parametric Sonar Transmitter Design," Proceedings of the British Acoustical Society Meeting on Nonlinear Acoustics, Birmingham, England, April 1971.

R. H. Mellen and M. B. Moffett, "A Model for Parametric Sonar Radiator Design," NUSC Technical Memorandum PA 4-229-71, 14 Sep. 1971.

M. B. Moffett, "Parametric Radiator Theory I," NUSC Technical Memorandum PA-4-234-71, 27 Sep. 1971.

T. G. Muir, "An Analysis of the Parametric Acoustic Array for Spherical Wave Fields," Applied Research Laboratory, Univeristy of Texas, Technical Report 71-1 (1971).

T. G. Muir and J. E. Blue, "Experiments on the Acoustic Modulation of Large-Amplitude Waves," J. Acoust. Soc. Amer. 46, 227-232 (1969).

J. Naze and S. Tjøtta, "Nonlinear Interaction of Two Sound Beams," J. Acoust. Soc. Amer. 37, 174-175 (L) (1965).

J. L. Nelson and L. F. Carlton, "A Parametric Sonar Echo Ranging Experiment," NUSC Technical Memorandum TDIX-6-72, 2 Mar. 1972.

B. V. Smith, "An Experimental Study of a Parametric End-Fire Array," J. Sound Vib. 14, 7-21 (1971).

P. J. Westervelt, "Parametric Acoustic Array," J. Acoust. Soc. Amer. 35, 535-537 (1963).

APPENDIX A
EFFECT OF DIRECT RADIATION

The importance of using a high-pass filter to block the difference-frequency component in the current from the power amplifier was not fully appreciated during the early experimentation. Consequently, the filter was not used at first, and several radiation patterns were obtained that reveal the presence of some direct radiation at the difference frequency, in addition to the parametirc radiation. During one test situation a driving current of 0.26 A in each primary was supplied, without filtering, to transducer E8#50. The driving current also contained a 50-kHz difference-frequency component of 6.8 mA. Direct radiation at 50 kHz by this current component produces a sound pressure level at 3.7 m that is 32 dB below the parametric radiation level at the same range, and about 90 dB below each primary *SPL* at the same range.

The effect of direct radiation on the polar radiation distribution patterns is shown in Figs. A1 and A2. These figures are a sequence of radiation patterns at ranges from 0.18 to 5.3 m of a parametrically generated difference-frequency beam of 50 kHz, including some direct 50-kHz radiation. The difference between these patterns and those in Fig. 4, where no direct radiation is present, is obvious. The sound pressure level of the direct radiation can be estimated from the plotted patterns. Direct 50-kHz radiation from a piston the size of the E8 transducer is down 3 dB at 50° off-axis. Referring, for example, to the pattern at 2.0 m in Fig. 4, one sees that the parametric radiation at 50° off-axis is below the axial level by more than 40 dB. In Fig. A2 the radiation level at 2.0 m and 50°, most of which is apparently due to direct radiation, is 29 dB below the axial level. The level of direct radiation on the axis, then, is 3 dB greater, or 26 dB below the total axial level. In other words, the direct radiation in this case is about 5% of the parametric radiation. The relative contribution of direct radiation is greater at closer range because as range decreases, the direct radiation increases faster than the parametric radiation. In the cases observed, direct radiation had little effect on the axial *SPL* or 3-dB beamwidth but significantly altered the off-axis portion of the radiation patterns, especially at close range.
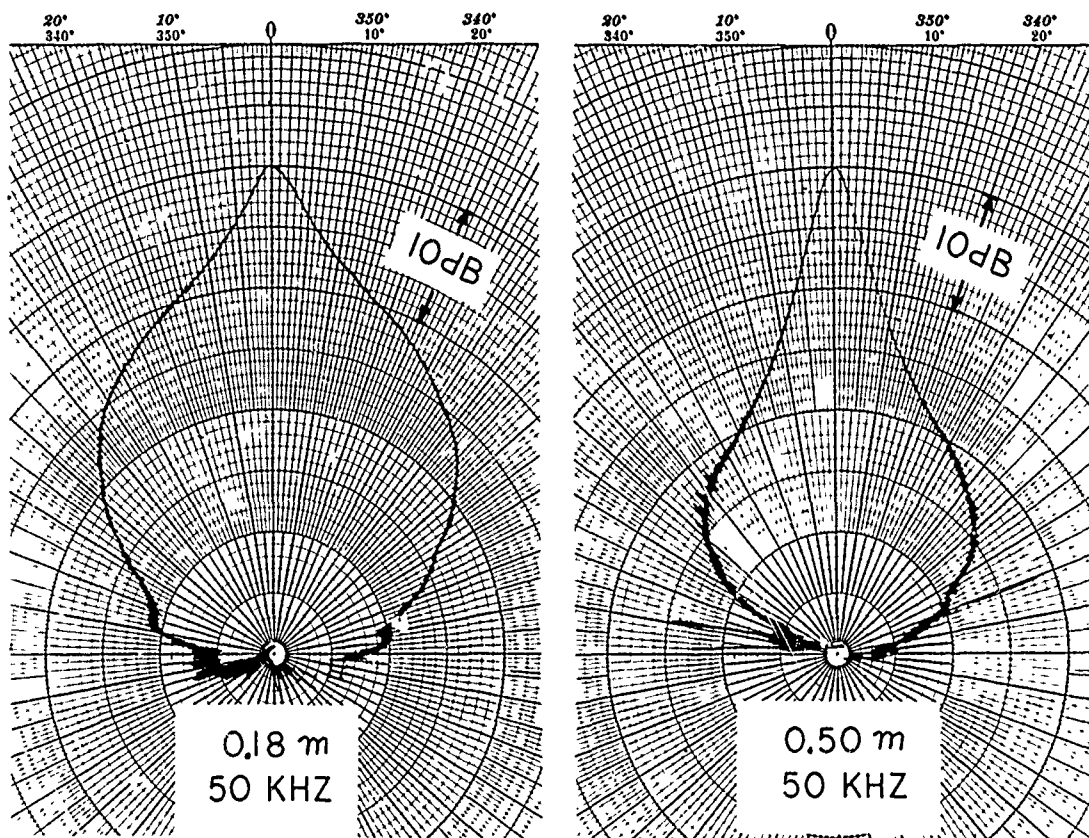
17

Fig. A1—Difference-frequency radiation patterns at 50 kHz for a sequence of ranges, including some direct radiation
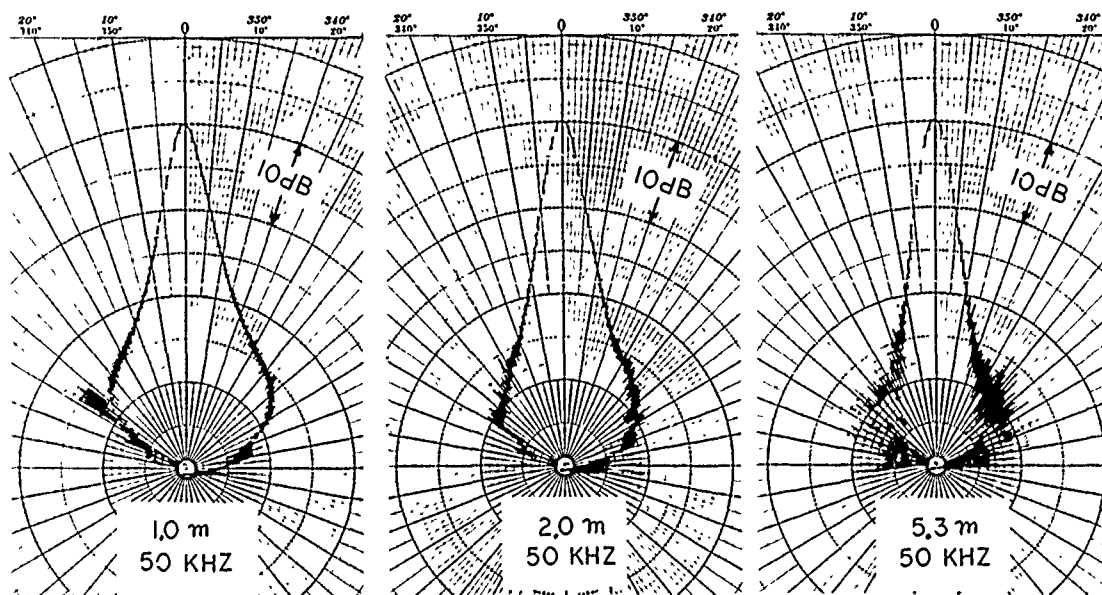
Fig. A2—Difference-frequency radiation patterns at 50 kHz for a sequence of ranges, including some direct radiation

By removing the rear plate of the bladder housing, substituting an open grille, and using helium as the compensating gas, it is possible to attain the transmitting current response 65 dB re 1 μbar/A at 47 Hz.

Conservation of Compensating Gas

Several tests were carried out to determine the amount of depth change that can be compensated by the rubber bladder alone. At the maximum depth 600 ft, the rubber bladder will provide compensation for a decrease in depth of 378 ft. The amount of compensation by the bladder is reduced with decrease in operating depth as shown in Fig. 9.
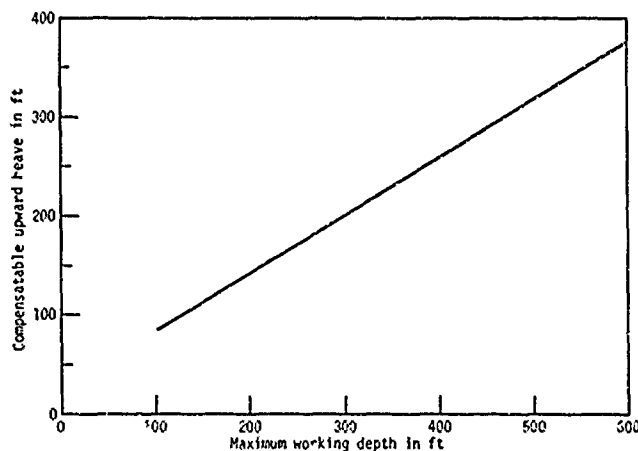
Fig. 9. Relation of compensatable upward heave to maximum working depth.

Calculations in Appendix B show that if the SCPCS gas supply is fully charged to start with, seven excursions can be made from the surface to 600 ft and back before it becomes necessary to replenish the gas supply. The amount of gas used from the bottle for each full depth excursion is based on the drop in bottle pressure recorded during tests in the pressure tank. Because of charging limitations, the highest gas-bottle pressure attainable during the tests was 1480 psig.

Maximum Pressure Differential

The maximum pressure differential that occurred within the transducer was not measured. The maximum value would occur during rapid descent to or ascent from operating depth, when the highest demands are made on the supply regulators and the relief valve. Maximum rates of descent and ascent during the tests were recorded, however. The highest rate of descent was 8.29 ft/sec; the highest ascent rate, 9.21 ft/sec. These rates were experienced without structural failure of the transducer.

CONCLUSION

This self-contained pressure-compensating system adequately replenishes compensating gas for the USRD type J11 transducer during a long period of submergence with little effect on the mechanical and acoustical operation of the transducer. Further development will be carried out to adapt the system for use with the USRD moving-coil transducers types J9 and J13.

References

1. C. C. Sims, "High-Fidelity Underwater Sound Transducers," Proc. IRE **47**, 866-871 (1959).

2. T. A. Henriquez, "Air-Compensated Audio Transducers for Operation to 500-Foot Depth," Navy Underwater Sound Reference Laboratory Research Report No. 80 (1966)[AD-627 383].

3. L. E. Kinsler and A. R. Frey, Fundamentals of Acoustics (John Wiley and Sons, New York, 1962), 2nd ed., pp. 187, 193.

Appendix A

ATTENUATION OF SOUND BETWEEN
HOUSING OF TRANSDUCER ELEMENT AND BLADDER HOUSING

Figure A1 shows the acoustical system considered in determining the sound transmission through the 2.54-mm-dia (0.100 in.) holes through the centers of the four bulkhead bolts leading from the housing of the transducer element to the bladder housing.
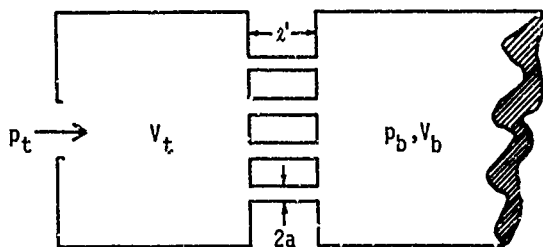

Fig. A1. Acoustical path between bladder housing and that of transducer element; V_t is volume of element housing; V_b is volume of bladder housing; a is radius and ℓ' the length of hole in each bolt.

Figure A2 shows the equivalent electrical circuit for this acoustical system. The elements C_t and C_b of the circuit are the volume compliances of volumes V_t and V_b, respectively, where $C_t = V_t/\rho_0 c^2$ and $C_b = V_b/\rho_0 c^2$; ρ_0 is the density of, and c is the sound speed in, the compensating gas; p_t and p_b are the sound pressures at the entrance to the transducer housing and the bladder housing, respectively.
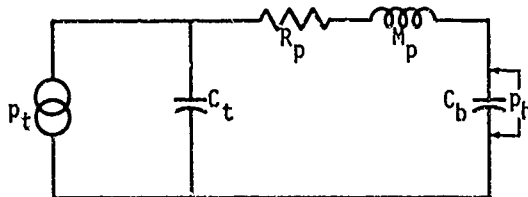

Fig. A2. Equivalent electrical circuit for acoustical path shown in Fig. A1.

For the boundary condition 16 Hz < f < 3900 Hz, the total acoustical resistance [A1] of the four passages is

$$R_p = \rho_0 (1/4\pi a^2)(2\omega\mu)^{\frac{1}{2}}(2 + \ell'/a),$$

and the acoustical inertance is

$$M_p = \rho_0 (\ell' + 2\ell'')/4\pi a^2,$$

where $\omega = 2\pi f$, μ is the kinematic coefficient of viscosity of the compensating gas, and $\ell'' = 0.85a$ is the end correction for the passage.

Applying network analysis to the equivalent electrical circuit, we find that

$$p_b/p_t = 1/[(1 - \omega^2 C_b M_p/4) + j(\omega C_b R_p/4)].$$

Numerical values for the worst condition (V_b maximum) and nitrogen gas are: $V_b = 0.00420 \, m^3$, $a = 0.00127 \, m$, $\ell' = 0.0476 \, m$, $c = 343 \, m/sec$, and $\mu = 1.56 \times 10^{-5}$. With these values, we get

$$p_b/p_t = 1/[(1 - 8.75 \times 10^{-5}\omega^2)^2 + (3.89 \times 10^{-4}\omega^{3/2})^2]^{\frac{1}{2}}.$$

For specific frequencies, the attenuation is:

Freq (Hz)	20 log (p_b/p_t) (dB)
50	-19
100	-34
3900	-127

Reference

A1. L. L. Beranek, Acoustics (McGraw-Hill Book Co., Inc., New York, 1954), pp. 137-138.

Appendix B

EXPENDITURE OF HIGH-PRESSURE GAS

To supply compensating gas to the low-pressure regulator at the depth 600 ft, the gas bottle pressure must be at least 347 psig, where the pressure gradient in seawater is 0.445 psi/ft and the pressure supplied to the low-pressure regulator is to be maintained at 80 psi above the hydrostatic pressure.

The total mass of compensating gas available from the high-pressure gas bottle before its initial pressure p_1 is reduced to the final allowable pressure p_2 is

$$m_t = V_g(\rho_1 - \rho_2),$$

where V_g is the volume of the gas bottle and ρ_1 and ρ_2 are the initial and final gas densities at pressures p_1 and p_2, respectively.

From the general law for perfect gases, $\rho_1 = p_1/RT$ and $\rho_2 = p_2/RT$, where T is absolute temperature and R is a constant depending on the units used. Then,

$$m_t = V_g(p_1 - p_2)RT;$$

but similarly, the mass of gas expended in one excursion from surface to the depth 600 ft is

$$m_e = V_g\Delta p/RT,$$

where Δp is the reduction in pressure of the gas in the storage bottle and, from measurement, is equal to 200 psi.

Then the number of excursions to 600 ft that can be made without replenishing the gas bottle is $m_t/m_e = (p_1 - p_2)/\Delta p$.

For the given conditions, p_1 is 1800 psig, p_2 is 347 psig, and m_t/m_e is approximately equal to seven excursions.